Dynamic light deflection in an active Raman-gain medium using a spatially inhomogeneous pump

Chengjie Zhu,[1,2] L. Deng,[1] and E. W. Hagley[1]
[1]*National Institute of Standards and Technology, Gaithersburg, Maryland 20899, USA*
[2]*East China Normal University, Shanghai, China*
(Received 17 April 2013; published 25 July 2013)

We study optical wave deflection in a three-level active Raman gain medium using a spatially inhomogeneous pump field. Using the eikonal approximation, we derive an analytical expression for the deflection angle and demonstrate more than an order of magnitude increase in deflection when compared to the electromagnetically induced transparency method. Numerical simulations have shown excellent agreement with semi-classical theoretical predictions. We further discuss the concept of light-beam-deflection-based wavelength division multiplexing which may have important applications in integrated circuits for optical telecommunications.

DOI: 10.1103/PhysRevA.88.013841 PACS number(s): 42.65.Dr, 42.50.Gy

I. INTRODUCTION

The control of light-wave propagation and optical beam trajectory in media has been an area of long-term interest of research since the dawn of optics. Using a glass prism, Newton [1] famously demonstrated light trajectory change in a homogeneous medium; a dispersion phenomenon that is based on the wavelength dependence of the material refractive index.

In the past decades, dynamic light beam deflection in a homogeneous medium subject to external fields has received considerable interest. Experimental observations [2–7] and theoretical investigations [8–10] have demonstrated and explained how dynamic light beam deflection can be achieved with external fields. In all studies reported to date only two methods have been used for the control of light deflection. Either an inhomogeneous external magnetic field [6] was used, or an inhomogeneous external optical pump field [7,11] was applied. Most of these studies, including the more recent works, rely on a Λ-type three-level atomic medium using an electromagnetically induced transparency (EIT) [12] technique to enhance the light beam deflection angle [6–10]. The motivation was based on the observation that the probe light deflection angle in such a Λ-type three-level atomic medium under EIT excitation is proportional to the material dynamic susceptibility which is inversely proportional to the EIT control field intensity. Correspondingly, as the control field is reduced the deflection angle increases.

In this work, we present a theoretical study of light deflection using an active Raman gain (ARG) medium excited by a spatially inhomogeneous pump laser. We demonstrate more than an order of magnitude increase in the deflection angle when compared to the typical deflection using EIT methods. We shown analytically under the eikonal approximation that very large light beam deflections can be achieved without the detrimental attenuation of the probe field that is commonly encountered in EIT-based schemes. We further carry out full probe-field propagation simulations over an extended propagation distance and show the excellent agreement with analytical results obtained with the eikonal approximation. We also discuss possible applications of this light-wave selection method in an on-chip wavelength selection environment, demonstrating the potential of the scheme in integrated circuit applications in optical telecommunications.

II. MODEL

We consider a room-temperature three-state atomic system where the energy of state $|j\rangle$ is denoted as $\hbar\omega_j$ [Fig. 1(a)]. An intense, spatially distributed pump field with a Gaussian profile of angular frequency ω_L couples the upper electronic state $|3\rangle$ to a fully occupied ground state $|1\rangle$ [13] with a large one-photon detuning $\delta_3 = \omega_L - (\omega_3 - \omega_1)$. A weak probe field of angular frequency ω_p couples state $|3\rangle$ to state $|2\rangle$ with a two-photon detuning $\delta_2 = \omega_L - \omega_p - (\omega_2 - \omega_1)$. In this three-level ARG system [14,15] $2\Omega_L$ and $2\Omega_p$ are the Rabi frequencies of the pump and probe fields, respectively. Under the electric-dipole and rotating-wave approximations, the interaction Hamiltonian is given by

$$\hat{H}_{\rm int} = -\hbar\delta_2|2\rangle\langle 2| - \hbar\delta_3|3\rangle\langle 3| - \hbar(\Omega_L|1\rangle\langle 3| + \Omega_p|2\rangle\langle 3| + \text{H.c.}), \tag{1}$$

yielding atomic response equations of motion

$$\left(i\frac{\partial}{\partial t} + d_2\right)A_2 + \Omega_p^* A_3 = 0, \tag{2a}$$

$$\left(i\frac{\partial}{\partial t} + d_3\right)A_3 + \Omega_L A_1 + \Omega_p A_2 = 0. \tag{2b}$$

Here A_j ($j = 1$ to 3) is the probability amplitude of the bare atomic state $|j\rangle$, $d_j = \delta_j + i\gamma_j$ with γ_j being the atomic decay rate of the state $|j\rangle$ ($j = 2,3$). The normalization condition for this closed system is $\sum_{j=1}^{3}|A_j|^2 = 1$. In our model we have chosen the $5P_{1/2}$ $F' = 3$ manifold of the ^{85}Rb atom as the upper excited state. The $5P_{1/2}$ $F' = 2$ manifold is about 360 MHz away and has a much weaker transition strength with a linearly polarized pump. With one-photon detuning $\delta_3/2\pi = 1$ GHz, the total contribution from the $5P_{1/2}$ $F' = 2$ manifold is only about 15% and hence is neglected.

In the linear regime, the probability amplitude of the atomic state can be derived using multi-order adiabatic theory. Taking $A_i = A_i^{(0)} + \lambda A_i^{(1)}$ ($i = 1,2,3$), where λ is a small parameter characterizing the interaction order and choosing, for the weak probe field, $\Omega_p = \lambda\Omega_p$ we obtain the following zeroth-order adiabatic solutions of Eqs. (2): $A_1^{(0)} = 1/\sqrt{1+|\Omega_L/d_3|^2}$, $A_3^{(0)} = -\Omega_L/(d_3\sqrt{1+|\Omega_L/d_3|^2})$, and $A_2^{(0)} = 0$. The first-order adiabatic solutions of the probability amplitude of the atomic states can thus be obtained by solving Eqs. (2)

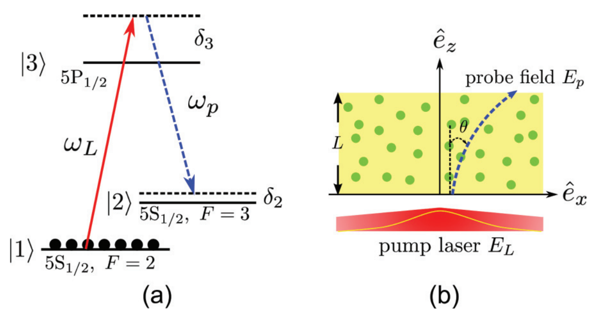

FIG. 1. (Color online) (a) ^{85}Rb three-level active Raman gain scheme with laser couplings. (b) Probe light deflection in an active Raman gain medium under a spatially distributed pump field.

iteratively, yielding the linear probe-field susceptibility

$$\chi_p^{(\mathrm{ARG})} = \frac{\mathcal{N}_a|\boldsymbol{p}_{23}|^2}{\varepsilon_0\hbar\Omega_p}A_3^{(0)}A_2^{*(1)} = -\frac{\mathcal{N}_a|\boldsymbol{p}_{23}|^2}{\varepsilon_0\hbar}\frac{|\Omega_L|^2}{(\delta_2 - i\gamma_2)(|d_3|^2+|\Omega_L|^2)}, \tag{3}$$

where $\mathcal{N}_a$ is the atomic density and $\boldsymbol{p}_{23}$ is the dipole moment of the $|3\rangle \leftrightarrow |2\rangle$ transition. The index of refraction for the probe field can be written as $n = \sqrt{1+\chi_p^{(\mathrm{ARG})}} = n' + in''$, where n' and n'' are the real and imaginary parts of the refractive index, respectively. Clearly, both n' and n'' become space dependent if the pump laser Ω_L has any spatial dependency. Consequently, both the probe light deflection angle and gain become spatially dependent.

The trajectory of the light rays traveling in an inhomogeneous medium, regardless of whether the inhomogeneity results from the density distribution, transverse magnetic field gradient, or the transverse distribution of the pump laser, can be studied using the eikonal approximation [16]. We start with the Maxwell equation that describes the propagation of the probe field

$$\nabla^2\tilde{E} - \frac{1}{c^2}\frac{\partial^2\tilde{E}}{\partial t^2} = \frac{1}{\varepsilon_0 c^2}\frac{\partial^2\tilde{P}}{\partial t^2}. \tag{4}$$

In most cases, we can expand the field and polarization in term of the slowly varying amplitudes $E_p(z,x)$ and the eikonal ϕ as

$$\tilde{E} = E_p \exp\left[i(k_p\phi - \omega_p t)\right] + \text{c.c.}, \tag{5a}$$

$$\tilde{P} = \mathcal{N}_a\{\boldsymbol{p}_{32}A_3A_2^* \exp\left[i(k_p\phi - \omega_p t)\right] + \text{c.c.}\}. \tag{5b}$$

Here $k_p = \omega_p/c$ with ω_p being the angular frequency of the probe field. If we neglect the second-order derivative over the z coordinate for the amplitude E_p, the eikonal equation is given by

$$(\nabla\phi)\cdot(\nabla\phi) = n'^2. \tag{6}$$

By defining $\nabla\phi = n' d\boldsymbol{R}/ds$ with the length variation $ds = \sqrt{dx^2+dy^2+dz^2}$, we obtain the well-known geometrical optics differential equation in vector form

$$\frac{d}{ds}\left(n'\frac{d\boldsymbol{R}}{ds}\right) = \nabla n'. \tag{7}$$

Here $\boldsymbol{R}(x,z) = X(z)\,\boldsymbol{e}_x + z\,\boldsymbol{e}_z$, with Cartesian coordinate unit vectors $\boldsymbol{e}_x$ and $\boldsymbol{e}_z$ in the y plane, defines a point on the light ray. In individual component form, Eq. (7) yields

$$\frac{d}{ds}\left(n'\frac{dX}{ds}\right) = \frac{\partial n'}{\partial x} \quad \text{and} \quad \frac{d}{ds}\left(n'\frac{dz}{ds}\right) = \frac{\partial n'}{\partial z}, \tag{8}$$

where, when $ds \approx dz$ for small deflections, the first equation reduces to an ordinary differential equation describing the ray trajectory

$$\frac{d^2X}{dz^2} = \frac{dn'}{dx}. \tag{9}$$

Using Eq. (9) the trajectory of the ray and the deflection angle θ can be estimated if we assume that the linear susceptibility is comparable to that at the incident point x_0. This results in a light deflection angle of

$$\theta \approx \left.\frac{dx}{dz}\right|_{z=L} \approx \left.\frac{dn'}{dx}\right|_{x=x_0} L, \tag{10}$$

where L is the medium length in the propagation direction [17].

To estimate the dynamic angle of defection caused by a spatially inhomogeneous pump field, we assume that the transverse distribution of the pump laser has a Gaussian profile

$$\Omega_L(x) = \Omega_L^{(0)}\exp\left(-x^2/\sigma_L^2\right), \tag{11}$$

where $\Omega_L^{(0)}$ is the peak Rabi frequency of the pump laser and σ_L is the $1/e$ radius of the transverse spot size. The refractive index is then given by

$$n'(x) \approx 1 - \frac{\mathcal{N}_a|\boldsymbol{p}_{23}|^2}{2\varepsilon_0\hbar}\frac{\left|\Omega_L^{(0)}\right|^2\delta_2}{\left(\delta_2^2+\gamma_2^2\right)|d_3|^2}e^{-2x^2/\sigma_L^2} \tag{12}$$

and the light deflection angle is

$$\theta_{\mathrm{ARG}} \approx \frac{2\mathcal{N}_a|\boldsymbol{p}_{23}|^2}{\varepsilon_0\hbar}\frac{\left|\Omega_L^{(0)}\right|^2\delta_2}{\left(\delta_2^2+\gamma_2^2\right)|d_3|^2\sigma_L^2}x_0L. \tag{13}$$

Notice that $\delta_2/(\delta_2^2+\gamma_2^2) \leqslant 1/2\gamma_2$ and $d_3 \approx \delta_3$, thus Eq. (13) has an upper bound of

$$\theta_{\mathrm{ARG}} < \frac{2\mathcal{N}_a|\boldsymbol{p}_{23}|^2\left|\Omega_L^{(0)}\right|^2}{\varepsilon_0\hbar\gamma_2|\delta_3|^2\sigma_L^2}x_0L. \tag{14}$$

III. COMPARISON WITH EIT SCHEMES

We now compare and contrast this ARG scheme to the widely studied three-level EIT scheme [6,7,9,10]. For a weak probe field, the linear susceptibility of the EIT medium can be express as [14,15]

$$\chi_p^{(\mathrm{EIT})} = \frac{\mathcal{N}_a|\boldsymbol{p}_{13}|^2}{\varepsilon_0\hbar}\frac{\delta_2+i\gamma_2}{|\Omega_C|^2-(\delta_3+i\gamma_3)(\delta_2+i\gamma_2)}, \tag{15}$$

where $2\Omega_C$ is the control field Rabi frequency. Assuming the same control field transverse Gaussian distribution, i.e., $\Omega_C(x) = \Omega_C^{(0)}\exp(-x^2/\sigma_C^2)$, the deflection angle of an EIT scheme under the condition of near transparency (i.e., $|\Omega_C| \gg \delta_2,\gamma_3$) is given by

$$\theta_{\mathrm{EIT}} \approx \frac{2\mathcal{N}_a|\boldsymbol{p}_{13}|^2}{\varepsilon_0\hbar\sigma_C^2}\frac{\delta_2}{\left|\Omega_C^{(0)}\right|^2}x_0L. \tag{16}$$

For an EIT system, the two-photon detuning must be set in the range of the transparency window to avoid significant absorption, i.e., $\delta_2 \ll |\Omega_C^{(0)}|^2/\gamma_3$. Therefore, the deflection angle is limited by

$$\theta_{\rm EIT} < \frac{2\mathcal{N}_a|\boldsymbol{p}_{13}|^2}{\varepsilon_0\hbar\gamma_3\sigma_C^2}x_0L. \quad (17)$$

This upper bound, which limits EIT methods to only very small deflection angles, has been verified both theoretically and experimentally [9,10]. Typically, this angle is only on the order of $\theta_{\rm EIT} \simeq 10^{-4}$ radian and this is exactly what has been reported in Ref. [7] both experimentally and numerically.

A comparison of Eq. (17) with Eq. (14) makes it immediately clear that the EIT scheme has a fixed upper bound, but the ARG scheme has a dynamically changeable upper bound. This fundamental difference between the two schemes is rooted in the fact that in an EIT scheme (such as in Refs. [7,11]) the probe wave operates in an *absorption* mode whereas in an ARG scheme it operates in a *stimulated emission* mode. The direct technical impact is thus the significant probe wave loss, intrinsically slow response time, and much smaller light beam deflection effect in the EIT scheme such as that used in Ref. [7]. For this reason, neither reducing the control field intensity nor increasing the medium density will meaningfully improve the performance in EIT-based systems. Furthermore, increasing the deflection angle by driving the EIT system weakly results in significant probe-field transverse spreading and thus inevitably introduces wavelength or channel smear (see later). These conclusions are common to all EIT-based processes.

To verify the above analysis, we performed a full numerical calculation by solving Eqs. (2) and (4) with parameters typical of those reported in the literature. Specifically, we consider a rubidium vapor with an atomic density of $\simeq 10^{12}$ cm^{-3}, $\boldsymbol{p}_{13} = \boldsymbol{p}_{23} = 3.5 \times 10^{-29}$ C·m, $\delta_3/2\pi = 1$ GHz, and $\delta_2/2\pi = 800$ kHz for the ARG scheme. For the purposes of comparison with EIT schemes, all parameters are the same except $\delta_3 = 0$ Hz. The transverse width of the Gaussian profile is taken to be $\sigma_L = \sigma_C = \sqrt{2}$ cm, and the cell length is $L = 7.5$ cm. To coarsely account the effect of Doppler broadened lines, we assume $\gamma_2/2\pi = 10$ kHz, $\gamma_3/2\pi = 600$ MHz [18].

In Fig. 2, we plot the deflection angle, the linear gain, and loss as functions of the pump field, coupling field, and the transverse position x for the ARG and EIT system, respectively. With our parameters the deflection angle with the ARG method [Fig. 2(a)] is more than ten times larger than that of the EIT method [Fig. 2(c)]. Accompanying this significant increase in deflection angle is a larger linear gain [Fig. 2(b)] that enhances the electric field during its propagation. This is to be contrasted with EIT schemes which suffer significant probe-field adsorption [Fig. 2(d)] as the deflection angle increases [Fig. 2(c)]. In other words, although the angle of deflection can be increased by decreasing the strength of the coupling field $\Omega_C^{(0)}$, it comes at the price of significant probe-field adsorption. Such constraints, however, do not exist in ARG systems. This prominently shows the superiority of the ARG method over EIT methods.

To numerically investigate probe-beam deflection and propagation characteristics, we begin with the probe-wave propagation equation given by [19]

$$\nabla^2 E_p + 2\nabla[E_p \cdot \nabla(\ln n)] + n^2k_p^2E_p = 0. \quad (18)$$

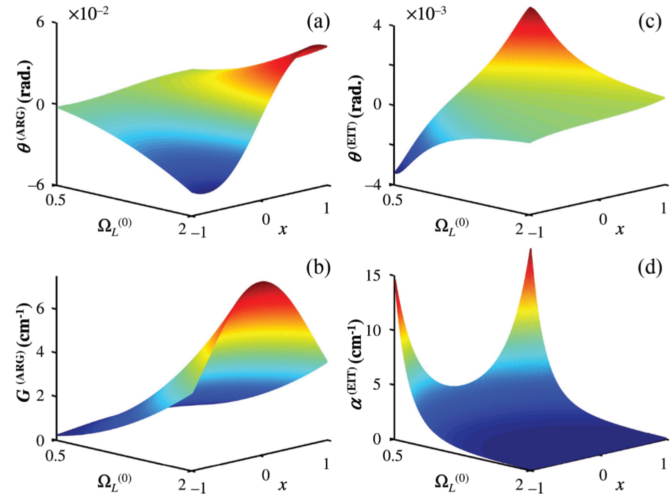

FIG. 2. (Color online) Deflection angle in (a) ARG and (c) EIT media as functions of the transverse position x (in units of cm) and the pump or coupling fields (in units of 100 MHz), respectively. (b) The resulting linear gain in the ARG scheme, and (d) the absorption in EIT systems is also plotted. Notice that with EIT methods strong absorption of the probe field is correlated with large light deflections.

Here n is the refractive index, which can be expressed as $n(x) = n_0 + \delta n(x)$ with $n_0 = 1$. Under the slow varying amplitude approximation, Eq. (18) can be written as

$$i\frac{\partial E_p}{\partial z} = \frac{1}{2n_0k_p}\left(\frac{\partial^2\delta n}{\partial x^2}E_p + 2\frac{\partial\delta n}{\partial x}\frac{\partial E_p}{\partial x} + \delta n\frac{\partial^2 E_p}{\partial x^2}\right) - \frac{1}{2k_p}\frac{\partial^2 E_p}{\partial x^2} - \frac{k_p\delta n}{n_0}E_p. \quad (19)$$

We numerically integrate Eq. (19) using a probe field with a transverse Gaussian intensity profile injected at various locations, i.e., $\Omega_p = \Omega_p^{(0)}\exp[(x-x_0)^2/\sigma_p^2]$. The probe beam width is characterized by $\sigma_p = 1$ mm and the probe incident

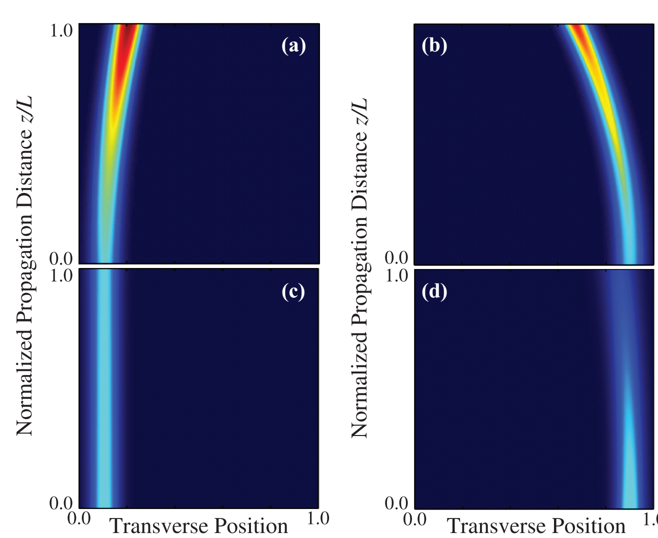

FIG. 3. (Color online) Numerical simulation of beam propagation in the (a,b) ARG and (c,d) EIT schemes. Probe injection locations: (a,c) $x_0 = 0.1$ cm and (b,d) 0.9 cm. The two-photon detunings are $\delta_2 = \pm\, 800$ kHz and $\Omega_L^{(0)} = \Omega_C^{(0)} = 100$ MHz.

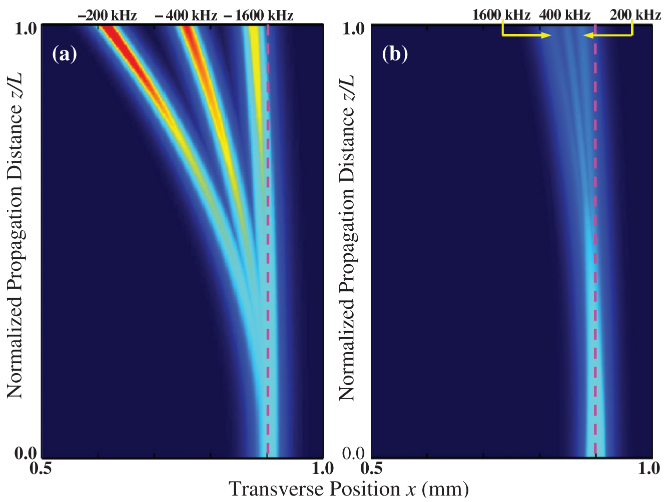

FIG. 4. (Color online) Angles of deflection of probe pulses with different wavelengths in (a) ARG and (b) EIT systems. Dashed line indicates the line of injection of the multifrequency probe light. Significant probe loss and channel smearing or cross-talk render occur under the EIT scheme, limiting its usefulness for such applications.

positions are $x_0 = 0.1$ and 0.9 cm, respectively, relative to the $x_0 = 0$ point which corresponds to the peak pump laser intensity [the pump field profile is given in Eq. (11)]. In the ARG medium, injection near the peak of the pump, $x_0 = 0.1$ cm, results in a 0.015 radian deflection angle accompanied with an increase in the probe beam intensity [Fig. 3(a)], On the other hand, when the probe is injected near the wing of the pump beam profile, a much larger deflection angle (nearly 0.03 rad) is obtained Fig. 3(b), and the wave-packet profile is well preserved during its propagation with only mild gain. However, the deflection angle with the EIT method is only $\simeq 10^{-4}$ radian for the incident position $x_0 = 0.1$ cm [Fig. 3(c)]. Although the deflection increases when $x_0 = 0.9$ cm, there is severe loss during its propagation because the driving field is significantly weaker at this location [Fig. 3(d)]. These results, which agree well with the analysis presented above, suggest that it is most effective to inject the probe near the wing or peak of the pump distribution for the ARG or EIT scheme, respectively.

The significant light-deflection angle in the ARG method could potentially be used to separate optical wavelengths for channel selection in wavelength division multiplexing (WDM) applications. To demonstrate the principle, we consider a frequency channeling device consisting of a slab ARG medium 2-mm wide and 7.5 mm in length. Let us assume that spot sizes of the pump and probe field are $\sigma_L = \sqrt{2}$ mm and $\sigma_p = 25$ μm, respectively. We further assume that the probe field has three frequency components so that, with a fixed pump-laser frequency, $\delta_2/2\pi = 200$, 400, and 1600 kHz, respectively. Taking $\Omega_L^{(0)}/2\pi = 100$ MHz and it is seen in Fig. 4(a) that the three components of the probe wave are well separated after a propagation distance of only 7.5 mm, indicating a well-isolated wavelength or channel selection operation is possible.

The EIT scheme, however, does not have these important advantages. Figure 4(b) shows the best compromise of angle deflection and probe field loss for three probe components in an EIT medium. Here, we take $\Omega_C^{(0)}/2\pi = 20$ MHz [all other parameters are the same as in Fig. 4(a)]. Channel smearing and cross-talk due to the small angle of deflection that is constrained by loss considerations render EIT schemes unpractical.

In conclusion, we have studied dynamic light deflection in a three-level active Raman gain medium using a spatially inhomogeneous pump laser. We present both analytical results using the eikonal equation for ray trajectories and full numerical simulations of the wave-propagation equation. We have shown a more than an order of magnitude increase in the light-beam deflection angle with ARG schemes when compared to the widely used EIT scheme. Furthermore, the detrimental probe field attenuation that is unavoidable with EIT schemes is completely eliminated in the ARG scheme. This important fact raises the real possibility of applications in telecommunications, such as the optical wave frequency channeling or selection scheme we discussed above. The clear separation of probe fields of different frequency demonstrates that ARG systems can be used in channel selection applications that are not possible under EIT methods.

[1] M. Born and E. Wolf, *Principles of Optics*, 7th (expanded) ed. (Cambridge University Press, Cambridge, England, 1999).
[2] R. Schlesser and A. Weis, Opt. Lett. **17**, 1015 (1992).
[3] R. Holzner, P. Eschle, S. Dangel, R. Richard, H. Schmid, U. Rusch, B. Rohricht, R. J. Ballagh, A. W. McCord, and W. J. Sandle, Phys. Rev. Lett. **78**, 3451 (1997).
[4] G. T. Purves, G. Jundt, C. S. Adams, and I. G. Hughes, Eur. Phys. J. D **29**, 433 (2004).
[5] R. R. Moseley, S. Shepherd, D. J. Fulton, B. D. Sinclair, and M. H. Dunn, Phys. Rev. Lett. **74**, 670 (1995).
[6] L. Karpa and M. Weitz, Nat. Phys. **2**, 332 (2006).
[7] V. A. Sautenkov, H. Li, Y. V. Rostovtsev, and M. O. Scully, Phys. Rev. A **81**, 063824 (2010).
[8] M. D. Lukin, Rev. Mod. Phys. **75**, 457 (2003).
[9] D. L. Zhou, L. Zhou, R. Q. Wang, S. Yi, and C. P. Sun, Phys. Rev. A **76**, 055801 (2007).
[10] Q. Sun, Y. V. Rostovtsev, and M. S. Zubairy, Phys. Rev. A **74**, 033819 (2006).
[11] It must be emphasized that the EIT-type of Raman process such as the one used in Ref. [7] and the ARG-type of Raman process studied in this work have fundamentally different characteristics. The former is based on the absorption of the probe field whereas the latter is based on stimulated emission in the probe mode.
[12] S. E. Harris, J. E. Field, and A. Imamoğlu, Phys. Rev. Lett. **64**, 1107 (1990).
[13] Such an initial state can be easily prepared using a combination of linear and circularly polarized light fields in a typical optical pumping scheme.

[14] L. Deng and M. G. Payne, Phys Rev Lett. **98**, 253902 (2007).

[15] C. J. Zhu, C. Hang, and G. X. Huang, Eur. Phys. J. D **56**, 231 (2010).

[16] K. V. Shajesh, *Eikonal Approximation*, Department of Physics and Astronomy, University of Oklahoma, http://www.nhn.ou.edu/∼shajesh/eikonal/sp.pdf.

[17] In general, the angle of deflection is small and we assume that the gradient of linear susceptibility is approximately the same as that of the incident point of the probe x_0.

[18] Typically, the two-photon relaxation rate in a warm vapor is about a few ten kHz. A probe pulse of about a few μs in duration will render the two-photon relaxation unimportant and the steady state treatment is well applicable.

[19] A. Ciattoni, P. D. Porto, B. Crosignani, and A. Yariv, J. Opt. Soc. Am. B **17**, 809 (2000).